Available online at www.sciencedirect.com
ScienceDirect
Journal of Solid State Chemistry 179 (2006) 3385–3393
JOURNAL OF SOLID STATE CHEMISTRY
www.elsevier.com/locate/jssc

Structural characterization of the Ta-rich part of the Ta–Al system

A. Boulineau[a], J.-M. Joubert[a,*], R. Černý[b]

[a]Laboratoire de Chimie Métallurgique des Terres Rares, CNRS, 2-8 rue Henri Dunant, F-94320 Thiais Cedex, France
[b]Laboratoire de Cristallographie, Université de Genève, 24 Quai Ernest Ansermet, CH-1211 Genève 4, Switzerland

Received 16 May 2006; received in revised form 22 June 2006; accepted 2 July 2006
Available online 7 July 2006

Abstract

The Ta-rich part of the Ta–Al system has been investigated. On the one hand, the accommodation of the non-stoichiometry in the σ phase has been studied by Rietveld refinement of X-ray powder data obtained from different samples on both sides of the ideal composition (Ta_2Al, $P4_2/mnm$, $tP30$). On the other hand, the structure of the β phase has been determined ab initio from powder synchrotron data (analyzed composition $Ta_{50.7}Al_{49.3}$, refined composition $Ta_{52.6(5)}Al_{47.4(5)}$ ($Ta_{45.2(4)}Al_{40.8(4)}$), stoichiometric composition $Ta_{48}Al_{38}$, $mP86$, $P2_1/c$, $a = 9.8707(1)$ Å, $b = 9.8766(1)$ Å, $c = 16.3539(2)$, $\beta = 116.478(1)$, $R_B = 2.6\%$). This phase is shown to be closely related to the group of the topologically close packed phases. In addition, phase relations have been accurately determined in the Ta-rich end of the system.

Keywords: Al–Ta; σ phase; Frank–Kasper phases; Intermetallic compound; Non-stoichiometry; Rietveld refinement; Ab initio powder structure determination

1. Introduction

The Ta–Al system has been subject of a lot of controversial reports [1–7]. The reasons for the discrepancies may be explained by the existence of a rather high number (6) of intermetallic compounds, their high structural complexity, the closeness in their composition, the difficulty in controlling the composition of the samples due to aluminum evaporation during synthesis and annealing treatments, and the absence of the use, except in rare cases, of analytical means such as electron probe microanalysis (EPMA). The most recent and accurate work has been published by Mahne et al. [5–7]. A compilation of the literature data is given in [8]. In the Ta-rich region ($x_{Ta} \geqslant 50$ at.%), two intermediate phases have been reported.

The σ phase is a topologically close packed (Frank–Kasper) phase. It has a tetragonal unit cell containing 30 atoms generated by the space group $P4_2/mnm$ from a basis of 5 atoms (CrFe structure type). These atoms are the centers of polyhedra of coordination numbers (CN) 12, 14 and 15 [9]. The σ phase is common in the binary systems of transition elements A–B with A belonging to the columns 5, 6 and 7 and B element belonging to the columns 7, 8, 9, 10 and 11. The structural data are given in Table 1 for the ordered σ phase in which A atom occupies the largest coordination sites and B atom the sites with CN 12. This model defines a stoichiometric composition A_2B. Though aluminum is not a transition element, it forms a σ phase and plays the role of a B element in the systems Ta–Al and Nb–Al [10]. A particularity of the σ phase is that it exists for concentration in A ranging from 10 at.% in the system V–Mn to 80 at.% in the system Ta–Ir. Moreover, it may have a large homogeneity domain in any given system. These two features indicate an ability to accommodate the variations of composition by a substitutional disorder on different sites. In the Ta–Al system, the reported composition ranges of the σ phase are, following the various authors 65–80 at.% Ta [1], 60–80 at.% Ta [2], 65–75 at.% Ta [3]. The only limit obtained from EPMA is the Ta-poor limit at 55.9 at.% Ta [4].

On the Ta-poor side, the σ phase is in equilibrium with a phase close to the equiatomic composition [5,7]. This phase has been named TaAl in previous work but due to

*Corresponding author. Fax: +33 1 49 78 12 11, +33 1 49 78 12 03.
E-mail address: jean-marc.joubert@glvt-cnrs.fr (J.-M. Joubert).

0022-4596/$ - see front matter © 2006 Elsevier Inc. All rights reserved.
doi:10.1016/j.jssc.2006.07.001

Table 1
Atomic positions for the ordered σ *A*–*B* phase at the composition A_2B

Atoms	Wyckoff position	*x*	*y*	*z*	CN
B	2*a*	0	0	0	12
A	4*f*	$x \approx 0.398$	*x*	0	15
A	$8i_1$	$x \approx 0.463$	$y \approx 0.132$	0	14
B	$8i_2$	$x \approx 0.737$	$y \approx 0.065$	0	12
A	8*j*	$x \approx 0.182$	*x*	$z \approx 0.252$	14

uncertainty about its composition and to avoid confusion between the phase name and its composition; it will be designated as β in the present work. It is reported to have a monoclinic structure with $a = 14.865$ Å, $b = 9.863$ Å, $c = 9.862$ Å and $\beta = 99.98$ [5]. The structure appears to be quite complex and has not been determined so far.

The aim of this work is to study by Rietveld refinement of powder X-ray diffraction (XRD) how the non-stoichiometry is accommodated in the σ phase. For this purpose, several samples across the homogeneity range have been synthesized and the atom distribution on the different sites has been refined. In a second step, the crystal structure of the β phase has been determined ab initio from synchrotron powder diffraction data. These two studies yield better description of the phase relations in the Ta–Al phase diagram.

2. Experimental

The samples were prepared either from powders of the pure elements (Ta: Alfa Aesar, −325 mesh, 99.97% (metals basis); Al: Alfa Aesar, −325 mesh, 99.97% (metals basis)) pressed into pellets or from pieces of the pure elements (Ta: Alfa Aesar, 99.95% (metals basis); Al: Alfa Aesar, 99.9965% (metals basis)). The pellets or the pieces were arc-melted under argon atmosphere during short time periods to limit aluminum evaporation related to its low boiling point, to the high melting point of Ta and to the high temperature of the arc. The alloys were melted several times to insure homogeneity. Finally, they were annealed to reach equilibrium in an induction furnace at 1460 °C during 7–9 h under argon atmosphere. The temperature was measured by an optical pyrometer and can be considered to be accurate at ±40 °C. One of the samples was annealed at lower temperature (1000 °C) during 7 days in a silica tube sealed under vacuum.

Though limited, Al evaporation losses have a strong influence on the atomic composition due to the high Ta content and to the huge difference in atomic weight between the two elements (a composition change of the order of 1 wt.% may result in a composition change as large as 5 at.%). For this reason, the alloys will not be designated after their nominal composition but rather after the analyzed composition (from EPMA for single-phase alloys, from EPMA and quantitative XRD for two-phase alloys).

The samples were characterized by conventional XRD, optical metallography and EPMA (Cameca SX100). For EPMA, pure metals were used as standards. The sum of the analyzed weight composition of each element was between 99.5 and 100.5 wt.% for each analysis point. A number of 20–100 analysis points were taken in each phase. The results presented are the average of the measurements together with standard deviations.

The diffraction patterns were collected at room temperature with a two circles D8 Advance (Bruker AXS) diffractometer in the $\theta-\theta$ Bragg–Brentano geometry (spinning sample, 2θ range 5–120°, step-scan intervals 0.04° (2θ) chosen according to the sample line widths, Cu $K\alpha$, backscattered rear graphite monochromator, scintillation detector).

The patterns were analyzed by Rietveld refinement with the program Fullprof [11]. For the σ phase (~230 reflections in the 2θ range), the occupancy parameters were refined considering the full occupancy of the 5 sites, possible atomic mixing of Ta and Al on each site and by constraining the overall composition to that measured by EPMA, i.e., 4 occupancy parameters were refined. The secondary phase, when present, was considered in the refinement with its proper crystal structure (i.e., with the presently determined structure for the β phase). Anisotropic line broadening was noted for the σ phase in several samples ($hk0$ broader than $00l$). Strains along *a*-axis were refined by using the strain model developed in Fullprof for the orthorhombic system and using the same parameter for the strains along *a* and *b*. For these samples, noticeable improvement of the refinements could be obtained as well by introducing preferential orientation along [001] direction (March's function, refined parameter close to 1.04 indicating a slight needle-like habit).

The synchrotron powder diffraction measurement was performed at room temperature on the sample $Ta_{49}Al_{51}$. Powder was prepared by crushing the button in an agate mortar. A glass capillary of diameter $2R = 0.3$ mm was chosen in order to maximize the diffracted intensity. The wavelength used was $\lambda = 0.37504$ Å.The $m\mu R$ value (μ is the linear absorption coefficient, *m* is the powder packing factor) was close to 1. The experiment was carried out on the Swiss–Norwegian beamline, at the ESRF, Grenoble, France, in Debye–Scherrer geometry (spinning sample, 2θ range 1–34°, step-scan intervals 0.0025° (2θ), primary Si monochromator, 6 detectors equipped with Si analyzer).

The structure of the β phase was solved ab initio by the global optimization of a structural model in direct space using the simulated annealing (in parallel tempering mode) and the recently developed program FOX [12]. The initial structure model was progressively refined by the combined use of Fourier difference maps and Rietveld refinement (~7300 reflections in the 2θ range used for refinement, effective number of reflections divided by the number of intensity parameters refined in the 'eclectic view' as defined by Fullprof: 11.8).

3. Results

3.1. Metallurgical characterization

The β phase in a nearly single-phase state, three σ single-phase samples at different compositions and three samples showing two-phase equilibrium between σ and β or bcc have been obtained. The compositions synthesized, annealing treatments and characterization including EPMA measurements are presented in Table 2.

3.2. Structure of the β phase

The synchrotron pattern of the sample $Ta_{49}Al_{51}$ was first refined without structural constraints (pattern matching) from the cell given by Mahne et al [5]. The following cell parameters were obtained for the β phase: $a = 14.8631(1)$ Å, $b = 9.8742(1)$ Å, $c = 9.8698(1)$ Å, $\beta = 100.004(1)^\circ$ which compare fairly well with those reported by Mahne et al. ($a = 14.865(3)$ Å, $b = 9.863(2)$ Å, $c = 9.862(2)$ Å, $\beta = 99.98(2)^\circ$). In order to determine the most probable space group, systematic extinctions were examined. Only one space group describes the extinction class observed: $P2_1/n$. The cell was converted to use the conventional space group $P2_1/c$. For the structure solution, the program Fox was used considering at first only the heavy atoms (Ta). When a sufficient number of these atoms was taken into account according to the estimated density and measured composition, aluminum atoms were introduced until all the excess Al atoms introduced into the model were systematically merged by the program. Fourier difference maps were calculated; highlighting the highest discrepancies between the electron density calculated from the model and that from the observed reflection intensities. According to this calculation, several atoms were changed in nature, added or suppressed. At this step, the structure model considered contained 12 Ta atoms and 9 Al atoms on general positions (4*e*), and 1 Al atom on a special position (2*c*).

This model was refined by Rietveld analysis. The peaks related to the presence of two secondary phases in minor quantities could be identified. These two phases are $Ta_{39}Al_{69}$, the structure of which is known from the literature [6] and the σ phase. They probably result from an incomplete peritectoid formation of the β phase. Only the first of these two phases could be identified from EPMA. Both were taken into account in the refinement. Much better results were obtained at low angles with interpolated background than with a refined polynomial one due to a complicated shape. It was therefore carefully interpolated though the severe overlap at high angles hinders an accurate description. Depending on the values taken for the background at high angles, the displacement parameters may change a lot. The absolute values of these parameters should therefore be taken with great care. However, significantly higher values of the displacement parameters of Ta compared to those of Al, together with a discrepancy between the model ($Ta_{48}Al_{38}$ i.e., $Ta_{55.8}Al_{44.2}$) and analyzed ($Ta_{50.7(2)}Al_{49.3(2)}$) compositions were indicative of a substitutional disorder on the Ta sites. Al substitution was refined on each site, yielding significant improvement of the agreement factors and a refined composition ($Ta_{52.6(5)}Al_{47.4(5)}$) in much better agreement with the analyzed one. Finally, a slight asymmetry was noticed at low angles and refined.

Table 2
Metallurgical characterization of the samples

Nominal composition (before melting)	Resulting composition (after synthesis)	Annealing treatment (temperature/time)	Phases	Composition (EPMA)	Phase amount (XRD) (wt.%)
$Ta_{49}Al_{51}$	$Ta_{49}Al_{51}$	1460 °C/8 h	β	$Ta_{50.7(2)}Al_{49.3(2)}$	90
			$Ta_{39}Al_{69}$ ($a = 19.172$ Å)	$Ta_{35.6(2)}Al_{64.2(2)}$	6
			σ ($a = 9.860$ Å, $c = 5.221$ Å)	Not analyzed	4
$Ta_{54}Al_{46}$	$Ta_{58}Al_{42}$	1460 °C/9 h	σ	$Ta_{60.1(7)}Al_{39.9(7)}$	35
			β ($a = 9.869$ Å, $b = 9.868$ Å, $c = 16.337$ Å, $\beta = 116.46^\circ$)	$Ta_{56.6(2)}Al_{43.4(2)}$	65
$Ta_{55}Al_{45}$	$Ta_{60}Al_{40}$	1000 °C/7 d	σ	$Ta_{61(1)}Al_{39(1)}$	92
			β (lattice parameters not refined)	$Ta_{52.9(3)}Al_{47.6(3)}$	8
$Ta_{60}Al_{40}$	$Ta_{65}Al_{35}$	1460 °C/8 h	σ	$Ta_{65(1)}Al_{35(1)}$	100
$Ta_{66}Al_{34}$	$Ta_{72}Al_{28}$	1460 °C/8 h	σ	$Ta_{72.4(9)}Al_{27.6(9)}$	100
$Ta_{67}Al_{33}$	$Ta_{74}Al_{26}$	1460 °C/7 h	σ	$Ta_{74(1)}Al_{26(1)}$	100
$Ta_{72}Al_{28}$	$Ta_{77}Al_{23}$	1460 °C/8 h	σ	$Ta_{76(1)}Al_{24(1)}$	96
			bcc ($a = 3.296$ Å)	$Ta_{\sim 98}Al_{\sim 2}$	4

The resulting composition is the one deduced from EPMA and phase amount determined by XRD. The samples are designated with this composition in the text.

In the final stage of the refinement, all the 63 atomic coordinates were refined together with 12 occupancy and 2 displacement parameters. The results are given in Table 3. The Rietveld plot is given in Fig. 1 and the structure is drawn in Fig. 2.

3.3. Accommodation of the non-stoichiometry across the homogeneity range of the σ phase

In agreement with previous studies on the σ phase [9,10], the presence of an homogeneity range was attributed to the substitutional disorder. The tantalum to aluminum ratios have been refined on each site considering no vacancy and a global constraint to the analyzed composition. The results are presented in Table 4 and drawn in Fig. 3 as a function of the composition across the homogeneity range. Close to the stoichiometric composition Ta_2Al ($Ta_{65}Al_{35}$), nearly complete order is observed, with tantalum occupying the sites of CN 14 and 15, and aluminum the sites of CN 12 in agreement with the relative atomic sizes and the crystal structure of the pure elements (preference for a bcc-like environment for Ta, and a fcc-like environment for Al). For compositions poorer in tantalum than the stoichiometry, aluminum substitutes on the sites occupied by tantalum and it can be noticed that the substitution occurs in larger amount on the site of CN 15. Contrary to the expectation, the tantalum site fraction on the two sites with CN 12 slightly increases with decreasing tantalum content. For compositions richer in tantalum than the stoichiometry, the sites with CN 14 and 15 tend to be completely occupied by tantalum, while the tantalum excess is located equally on the two sites with CN 12.

The cell parameters and the cell volume are plotted in Fig. 4 and 5. These figures are complemented with the value of the cell parameters for pure Ta in the structure of the σ phase (a metastable form of Ta [13]). A plot of the atomic coordinates (not shown) does not exhibit any significant variation of these parameters as a function of composition.

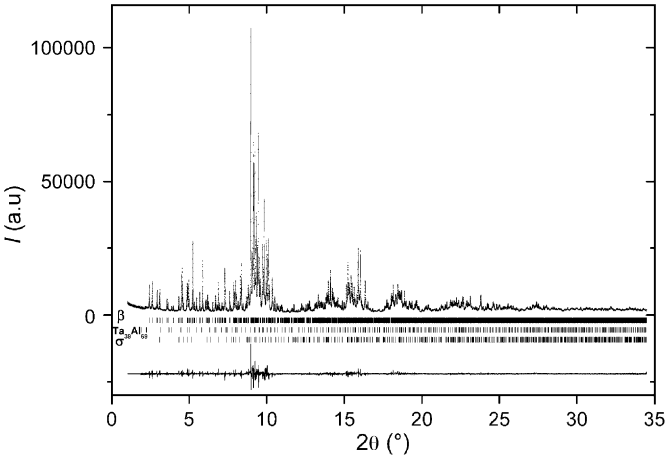

Fig. 1. Rietveld plot of the sample $Ta_{49}Al_{51}$ (synchrotron data, $\lambda = 0.37504$ Å). Observed (dots), calculated (line), difference (line below) curves are shown. Ticks represent reflections of the different phases.

Table 3
Crystal structure of the β phase in the sample

Atom	Wyckoff position	x	y	z	Occupancy	CN
Ta 1	4e	0.0524(3)	0.3777(2)	0.2196(2)	4.01(3)/Al -0.01(3)	16
Ta 2	4e	0.0758(3)	0.2734(2)	0.0192(2)	3.59(3)/Al 0.41(3)	14
Ta 3	4e	0.1039(3)	0.0986(2)	0.1842(2)	3.85(3)/Al 0.15(3)	14
Ta 4	4e	0.1546(3)	0.8424(2)	0.1657(2)	3.75(3)/Al 0.25(3)	14
Ta 5	4e	0.1822(3)	0.4206(2)	0.4123(2)	3.86(3)/Al 0.14(3)	14
Ta 6	4e	0.2130(3)	0.5697(2)	0.1392(1)	3.95(3)/Al 0.05(3)	16
Ta 7	4e	0.3172(3)	0.0574(2)	0.0913(2)	3.86(3)/Al 0.14(3)	14
Ta 8	4e	0.3518(3)	0.3447(2)	0.0304(2)	3.91(3)/Al 0.09(3)	15
Ta 9	4e	0.4593(3)	0.0144(2)	0.2771(2)	3.85(3)/Al 0.15(3)	15
Ta 10	4e	0.5406(3)	0.1392(2)	0.0128(2)	3.76(3)/Al 0.24(3)	15
Ta 11	4e	0.7184(2)	0.4309(2)	0.1364(2)	3.66(3)/Al 0.34(3)	15
Ta 12	4e	0.8203(3)	0.2038(2)	0.0232(2)	3.21(3)/Al 0.79(3)	14
Al 1	4e	0.0701(15)	0.1526(13)	0.3532(10)	4	12
Al 2	4e	0.1685(14)	0.6607(13)	0.3037(10)	4	12
Al 3	4e	0.3080(15)	0.3004(14)	0.1865(10)	4	12
Al 4	4e	0.3180(16)	0.2109(13)	0.3456(9)	4	12
Al 5	4e	0.3714(16)	0.4758(13)	0.3316(9)	4	12
Al 6	4e	0.5663(16)	0.1042(15)	0.4571(10)	4	12
Al 7	4e	0.5762(16)	0.2238(12)	0.1909(9)	4	12
Al 8	4e	0.5970(15)	0.2890(13)	0.3545(9)	4	12
Al 9	4e	0.8927(15)	0.4643(13)	0.0387(9)	4	11
Al 10	2a	0	0	0	2	12

$Ta_{49}Al_{51}$ (refined composition $Ta_{52.6(5)}Al_{47.4(5)}$ ($Ta_{45.2(4)}Al_{40.8(4)}$), stoichiometric composition $Ta_{48}Al_{38}$, *mP*86, $P2_1/c$, $a = 9.8707(1)$ Å, $b = 9.8766(1)$ Å, $c = 16.3539(2)$, $\beta = 116.478(1)$, $B_{Al1-Al10} = 0.13(6)$, $B_{Ta1-Ta12} = 0.301(3)$, $R_B = 2.6\%$, $\chi^2 = 6.2$).

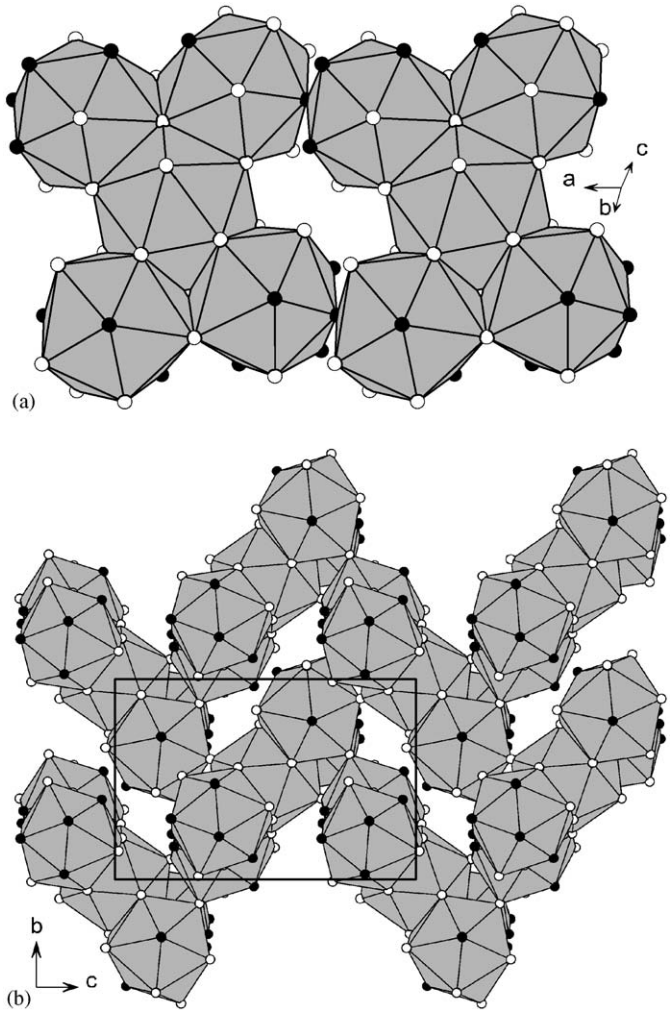

Fig. 2. Building block of the crystal structure of β phase (a) composed from five Al 1, Al 8 and Al 10 icosahedra in a close-packed configuration and forming chains along the *a*-axis by sharing vertices; (b) the chains are stacked in a zig-zag arrangement along the *c*-axis. Ligand atoms: Ta as white and Al as black spheres, mixed sites considered as Ta occupied.

4. Discussion

4.1. Structure of the β phase

The binary β phase crystallizes with a peculiar new monoclinic structure type, space group $P2_1/c$, Pearson symbol $mP86$. It contains 12 crystallographically independent tantalum and 10 aluminum sites.

Atoms of the first coordination sphere of each site are listed in Table 5. An analysis of the distances shows that all the tantalum atoms are at centers of polyhedra of CN 14, 15 and 16, and that all the aluminum atoms are centers of polyhedra of CN 12, but one (Al 9) which has a CN 11. The nearly exclusive presence of Frank–Kasper polyhedra makes the β phase a close representative of the group of the topologically close packed structures. As usual for these phases, and as it is the case for the σ phase, tantalum prefers the sites with high CN, while aluminum prefers the sites of CN 12.

The rules governing the polyhedral coordination in Frank–Kasper phases cannot be satisfied here for all atoms due to the number of atomic sites of Al and Ta. Therefore, the structure is probably stabilized by the deviation of the coordination of Al 9. Such a feature is observed for the Frank–Kasper related χ phase, which contains one atom with CN 13.

The interatomic distances in the structure are in some cases shorter than the sum of the atomic radii. The minimum distances observed are as follows (compared with the sum of the atomic radii between parentheses): Ta–Ta: 2.62 Å (2.98 Å); Ta–Al: 2.64 Å (2.92 Å); Al–Al:2.48 Å (2.86 Å). However, a contraction of a similar order of magnitude is observed in the σ phase and is not exceptional with intermetallic compounds.

The compound shows a small homogeneity domain (from 50.7 to 56.6 at.% Ta). Substitutional disorder has

Table 4
Structural characterization of the σ phase

Sample	$Ta_{58}Al_{42}$	$Ta_{60}Al_{40}$	$Ta_{65}Al_{35}$	$Ta_{72}Al_{28}$	$Ta_{74}Al_{26}$	$Ta_{77}Al_{23}$
Composition	$Ta_{60}Al_{40}$	$Ta_{61}Al_{39}$	$Ta_{65}Al_{35}$	$Ta_{72.4}Al_{27.6}$	$Ta_{74}Al_{26}$	$Ta_{76}Al_{24}$
2*a* (0, 0, 0)	Ta 0.12(3)	Ta 0.10(2)	Ta 0.07(1)	Ta 0.34(1)	Ta 0.42(1)	Ta 0.63(1)
CN 12						
4*f* (*x*, *x*, 0)	$x = 0.3990(4)$	$x = 0.3974(3)$	$x = 0.3985(2)$	$x = 0.3974(1)$	$x = 0.3972(1)$	$x = 0.3967(2)$
CN 15	Ta 3.24(3)	Ta 3.15(2)	Ta 3.80(2)	Ta 4	Ta 4	Ta 3.87(2)
$8i_1$ (*x*, *y*, 0)	$x = 0.4647(4)$	$x = 0.4629(2)$	$x = 0.4642(2)$	$x = 0.4640(1)$	$x = 0.4648(1)$	$x = 0.4645(1)$
CN 14	$y = 0.1336(4)$	$y = 0.1319(2)$	$y = 0.1300(2)$	$y = 0.1298(1)$	$y = 0.1301(1)$	$y = 0.1291(1)$
	Ta 7.20(5)	Ta 7.33(3)	Ta 7.82(2)	Ta 8.01(2)	Ta 8	Ta 7.70(2)
$8i_2$ (*x*, *y*, 0)	$x = 0.7473(18)$	$x = 0.7390(13)$	$x = 0.7415(11)$	$x = 0.7419(6)$	$x = 0.7424(4)$	$x = 0.7394(4)$
CN 12	$y = 0.0606(19)$	$y = 0.0718(14)$	$y = 0.0652(11)$	$y = 0.0646(6)$	$y = 0.0671(4)$	$y = 0.0672(4)$
	Ta 0.39(5)	Ta 0.39(4)	Ta 0.22(4)	Ta 1.31(2)	Ta 1.79(1)	Ta 2.74(2)
8*j* (*x*, *x*, *z*)	$x = 0.1802(3)$	$x = 0.1806(2)$	$x = 0.1810(1)$	$x = 0.1808(1)$	$x = 0.1807(1)$	$x = 0.1811(1)$
CN 14	$z = 0.2524(8)$	$z = 0.2511(5)$	$z = 0.2516(4)$	$Z = 0.2529(3)$	$z = 0.2524(3)$	$z = 0.2524(4)$
	Ta 7.09(5)	Ta 7.33(4)	Ta 7.69(3)	Ta 8.06(4)	Ta 8	Ta 7.78(2)
a (Å)	9.842(1)	9.845(1)	9.891(1)	9.942(1)	9.957(1)	10.014(1)
c (Å)	5.217(1)	5.217(1)	5.198(1)	5.198(1)	5.199(1)	5.211(1)
R_B (%)	5.5	9.7	4.7	3.7	4.8	4.8

Tantalum occupancies are indicated in atom per site, the complement to full occupancy is made by Al.

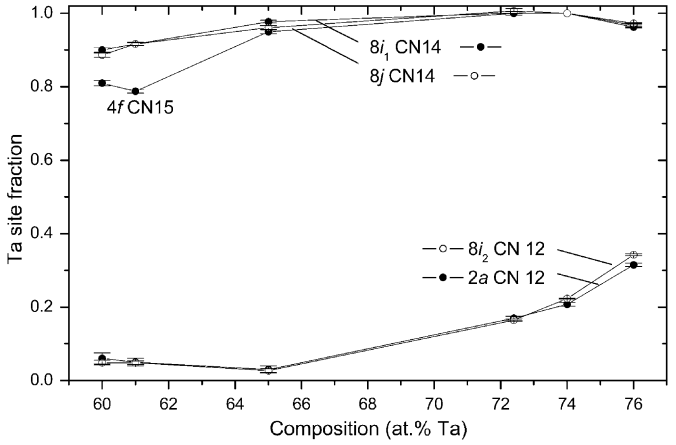

Fig. 3. Ta site fractions on the different sites of the σ phase as a function of composition. All the sites are fully occupied; Al complements Ta on each site.

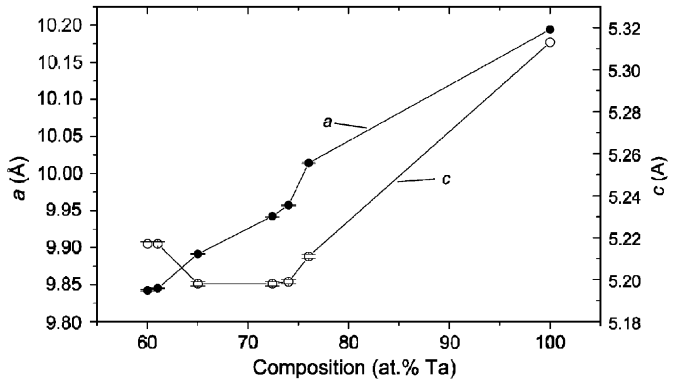

Fig. 4. Lattice parameters of the σ phase as a function of composition. The points at 100 at.% Ta refers to the metastable σ phase form of Ta [13].

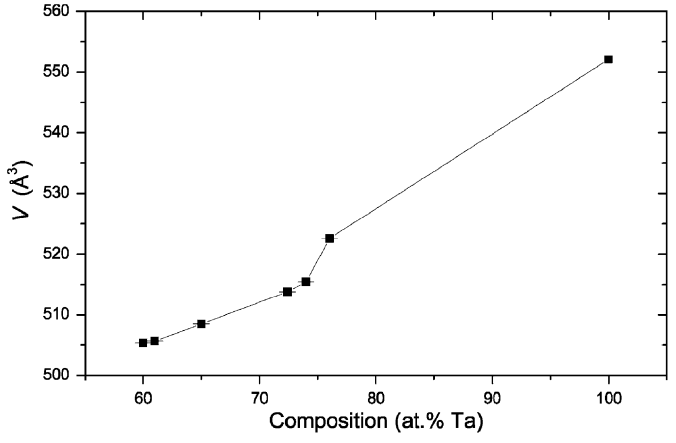

Fig. 5. Cell volume of the σ phase as a function of composition. The point at 100 at.% Ta refers to the metastable σ phase form of Ta [13].

been evidenced for the peculiar (Ta-poor) composition we have studied. The same model as for the σ phase occurs, i.e., a substitution of Al on Ta sites. This is indeed a typical feature of Frank–Kasper phases. One should observe that the substitution is not significant on the two sites with CN 16 and is the highest on one site of CN 14, respecting, to some extent, the size criterion. Interestingly, the composition of the β phase measured in the sample $Ta_{58}Al_{42}$ is $Ta_{56.6}Al_{43.4}$ very close to the stoichiometric composition resulting from the ordered model.

It is quite difficult to relate the crystal structure of the β phase with structures of other known intermetallic compounds. However, it can be rationalized as constructed from building blocks composed from five Al 1, Al 8 and Al 10 icosahedra in a close-packed configuration (Fig. 2a). The blocks form chains along the a-axis by sharing vertices. The chains are then stacked in a zig-zag arrangement along the c-axis (Fig. 2b).

4.2. Accommodation of the non-stoichiometry of the σ phase across the homogeneity domain

A situation close to full order is observed at the stoichiometric composition with tantalum located in the sites of CN 14 and 15 and aluminum occupying the two sites of CN 12. Limited anti-site defects exist possibly related to thermal disorder. Such a high-order cannot solely be explained by the atom radius difference ($R_{Ta} = 1.49$ Å, $R_{Al} = 1.43$ Å) but rather by the different electronic properties. Note that the σ phase at similar compositions is not always as ordered (e.g., in Cr–Ru and Cr–Os systems [14]). The model proposed by Edshammar and Holmberg [15] in their study of the stoichiometric composition is therefore fully correct though the substitutional disorder was not considered in this work.

For the compositions richer in tantalum, this element substitutes aluminum in the sites of low coordination as soon as the sites of high coordination are fully occupied. Such a mechanism is observed, for example, in σ Nb–Al [16].

For the compositions poorer in tantalum, this element is replaced by aluminum on the high CN sites. Unexpectedly, aluminum substitution is twice more pronounced for the site with the highest CN. It is contrary to the tendency for this element to locate preferentially on the sites of low CN. Even more unexpected is the evidencing of the slight increase of the tantalum occupancy on the two sites with CN 12. In addition, the c parameter shows an increase when tantalum concentration decreases. This feature was already noticed in previous work [17,18]. This is in apparent contradiction with the volume dependence as a function of composition, which is in agreement with the relative atomic sizes of Ta and Al. This feature may be understood in the frame of the steric relationships existing in the cell. One should first notice the extremely short distance between two tantalum atoms in site 8j ($\sim c/2$ i.e., 13% below tantalum diameter). The replacement of tantalum by aluminum occurring mainly in the 4f position, this has for a consequence a decrease of the a parameter. This results in a strong shrinkage of the hexagon in the basal plane as shown in Fig. 6. The distances between

Table 5
Atomic distances (in Å) below 4 Å in β Ta–Al phase

Ta 1	–Al 1	3.067(14)	Ta 2	–Al 1	2.787(16)	Ta 3	–Al 1	2.977(17)
	–Al 1	2.994(13)		–Al 3	2.685(11)		–Al 2	2.848(16)
	–Al 2	3.101(13)		–Al 9	2.727(15)		–Al 3	2.822(15)
	–Al 2	2.957(14)		–Al 9	2.823(14)		–Al 4	2.774(12)
	–Al 3	2.909(17)		–Al 10	2.782(2)		–Al 10	2.883(2)
	–Al 4	3.002(12)		–Ta 1	3.541(4)		–Ta 1	2.908(3)
	–Al 5	3.012(13)		–Ta 3	3.109(3)		–Ta 1	3.432(4)
	–Al 9	2.795(13)		–Ta 4	3.080(3)		–Ta 2	3.109(3)
	–Ta 2	3.541(4)		–Ta 5	3.077(4)		–Ta 4	2.623(3)
	–Ta 3	2.908(3)		–Ta 6	3.446(3)		–Ta 5	3.095(2)
	–Ta 3	3.432(4)		–Ta 6	3.264(3)		–Ta 7	3.123(4)
	–Ta 4	3.351(4)		–Ta 7	3.019(3)		–Ta 9	3.249(3)
	–Ta 5	2.855(3)		–Ta 8	2.740(4)		–Ta 11	3.137(3)
	–Ta 6	3.115(4)		–Ta 12	2.643(4)		–Ta 12	3.045(3)
	–Ta 11	2.999(3)						
	–Ta 12	3.457(3)						
Ta 4	–Al 1	2.814(14)	Ta 5	–Al 1	2.865(13)	Ta 6	–Al 1	2.968(16)
	–Al 2	2.841(15)		–Al 2	2.928(14)		–Al 2	3.051(16)
	–Al 7	2.894(12)		–Al 4	2.928(16)		–Al 3	2.811(14)
	–Al 8	2.668(17)		–Al 5	2.780(18)		–Al 5	2.970(13)
	–Al 10	2.8990(19)		–Al 10	2.865(3)		–Al 6	3.225(19)
	–Ta 1	3.351(4)		–Ta 1	2.855(3)		–Al 7	3.035(12)
	–Ta 2	3.080(3)		–Ta 2	3.077(4)		–Al 8	2.836(14)
	–Ta 3	2.623(3)		–Ta 3	3.095(2)		–Al 9	3.024(13)
	–Ta 5	3.081(3)		–Ta 4	3.081(3)		–Al 9	2.637(14)
	–Ta 6	2.828(3)		–Ta 7	2.630(3)		–Ta 1	3.115(4)
	–Ta 7	3.210(4)		–Ta 8	3.242(3)		–Ta 2	3.446(3)
	–Ta 9	3.219(3)		–Ta 10	3.265(3)		–Ta 2	3.264(3)
	–Ta 11	3.032(3)		–Ta 10	3.222(2)		–Ta 4	2.828(3)
	–Ta 12	3.239(4)		–Ta 12	2.994(3)		–Ta 8	3.487(3)
							–Ta 9	2.947(3)
							–Ta 12	3.374(3)
Ta 7	–Al 3	2.883(15)	Ta 8	–Al 1	2.990(11)	Ta 9	–Al 3	3.230(13)
	–Al 5	2.868(15)		–Al 3	2.807(17)		–Al 3	2.980(14)
	–Al 7	2.860(13)		–Al 4	2.940(16)		–Al 4	2.893(16)
	–Al 8	2.803(13)		–Al 6	2.669(15)		–Al 5	2.956(19)
	–AL 10	2.861(3)		–Al 6	2.904(19)		–Al 6	2.793(16)
	–Ta 2	3.019(3)		–Al 7	2.836(12)		–Al 7	3.007(16)
	–Ta 3	3.123(4)		–Al 9	2.869(13)		–Al 7	2.967(13)
	–Ta 4	3.210(4)		–Ta 2	2.740(4)		–Al 8	3.046(13)
	–Ta 5	2.630(3)		–Ta 5	3.242(3)		–Al 8	2.972(14)
	–Ta 8	3.076(3)		–Ta 6	3.487(3)		–Ta 3	3.249(3)
	–Ta 9	2.752(3)		–Ta 7	3.076(3)		–Ta 4	3.219(3)
	–Ta 10	3.113(4)		–Ta 9	3.312(3)		–Ta 6	2.947(3)
	–Ta 10	3.282(4)		–Ta 10	2.855(3)		–Ta 7	2.752(3)
	–Ta 12	3.121(3)		–Ta 11	3.351(2)		–Ta 8	3.312(3)
				–Ta 11	3.339(3)		–Ta 11	2.823(4)
Ta 10	–Al 2	3.100(11)	Ta 11	–Al 1	2.978(14)	Ta 12	–Al 2	2.814(16)
	–Al 4	3.023(12)		–Al 2	2.890(13)		–Al 6	2.938(15)
	–Al 5	2.804(14)		–Al 4	2.822(13)		–Al 8	2.654(11)
	–Al 5	2.906(13)		–Al 6	3.056(14)		–Al 9	2.652(13)
	–Al 6	2.742(16)		–Al 6	2.655(14)		–AL 10	2.818(3)
	–Al 7	2.896(15)		–Al 7	2.840(15)		–Ta 1	3.457(3)
	–Al 8	2.966(17)		–Al 9	2.842(18)		–Ta 2	2.643(4)
	–Ta 5	3.265(3)		–Ta 1	2.999(3)		–Ta 3	3.045(3)
	–Ta 5	3.222(2)		–Ta 3	3.137(3)		–Ta 4	3.239(4)
	–Ta 7	3.113(4)		–Ta 4	3.032(3)		–Ta 5	2.994(3)
	–Ta 7	3.282(4)		–Ta 8	3.351(2)		–Ta 6	3.374(3)
	–Ta 8	2.855(3)		–Ta 8	3.339(3)		–Ta 7	3.121(3)
	–Ta 10	2.842(3)		–Ta 9	2.823(4)		–Ta 10	2.764(4)
	–Ta 11	3.508(3)		–Ta 10	3.508(3)		–Ta 11	3.337(4)
	–Ta 12	2.764(4)		–Ta 12	3.337(4)			

Table 5 (*continued*)

Al 1	–Al 2	2.598(15)	Al 2	–Al 1	2.598(15)	Al 3	–Al 4	2.71(2)
	–Al 4	2.57(2)		–Al 5	2.598(20)		–Al 5	2.776(20)
	–Al 9	2.478(19)		–Al 7	2.56(2)		–Al 7	2.72(2)
	–Ta 1	3.067(14)		–Ta 1	3.101(13)		–Al 8	2.954(16)
	–Ta 1	2.994(13)		–Ta 1	2.957(14)		–Ta 1	2.909(17)
	–Ta 2	2.787(16)		–Ta 3	2.848(16)		–Ta 2	2.685(11)
	–Ta 3	2.977(17)		–Ta 4	2.841(15)		–Ta 3	2.822(15)
	–Ta 4	2.814(14)		–Ta 5	2.928(14)		–Ta 6	2.811(14)
	–Ta 5	2.865(13)		–Ta 6	3.051(16)		–Ta 7	2.883(15)
	–Ta 6	2.968(16)		–Ta 10	3.100(11)		–Ta 8	2.807(17)
	–Ta 8	2.990(11)		–Ta 11	2.890(13)		–Ta 9	3.230(13)
	–Ta 11	2.978(14)		–Ta 12	2.814(16)		–Ta 9	2.980(14)
Al 4	–Al 1	2.57(2)	Al 5	–Al 2	2.598(20)	Al 6	–Al 4	2.542(18)
	–Al 3	2.71(2)		–Al 3	2.776(20)		–Al 6	3.09(2)
	–Al 5	2.698(19)		–Al 4	2.698(19)		–Al 8	2.59(2)
	–Al 6	2.542(18)		–Al 7	2.562(18)		–Al 9	2.964(20)
	–Al 8	2.80(2)		–Al 8	2.79(2)		–Ta 6	3.225(19)
	–Ta 1	3.002(12)		–Ta 1	3.012(13)		–Ta 8	2.669(15)
	–Ta 3	2.774(12)		–Ta 5	2.780(18)		–Ta 8	2.904(19)
	–Ta 5	2.928(16)		–Ta 6	2.970(13)		–Ta 9	2.793(16)
	–Ta 8	2.940(16)		–Ta 7	2.868(15)		–Ta 10	2.742(16)
	–Ta 9	2.893(16)		–Ta 9	2.956(19)		–Ta 11	3.056(14)
	–Ta 10	3.023(12)		–Ta 10	2.804(14)		–Ta 11	2.655(14)
	–Ta 11	2.822(13)		–Ta 10	2.906(13)		–Ta 12	2.938(15)
Al 7	–Al 2	2.56(2)	Al 8	–Al 3	2.954(16)	Al 9	–Al 1	2.478(19)
	–Al 3	2.72(2)		–Al 4	2.80(2)		–Al 6	2.964(20)
	–Al 5	2.562(18)		–Al 5	2.79(2)		–Al 9	3.00(2)
	–Al 8	2.67(2)		–Al 6	2.59(2)		–Ta 1	2.795(13)
	–Ta 4	2.894(12)		–Al 7	2.67(2)		–Ta 2	2.727(15)
	–Ta 6	3.035(12)		–Ta 4	2.668(17)		–Ta 2	2.823(14)
	–Ta 7	2.860(13)		–Ta 6	2.836(14)		–Ta 6	3.024(13)
	–Ta 8	2.836(12)		–Ta 7	2.803(13)		–Ta 6	2.637(14)
	–Ta 9	3.007(16)		–Ta 9	3.046(13)		–Ta 8	2.869(13)
	–Ta 9	2.967(13)		–Ta 9	2.972(14)		–Ta 11	2.842(18)
	–Ta 10	2.896(15)		–Ta 10	2.966(17)		–Ta 12	2.652(13)
	–Ta 11	2.840(15)		–Ta 12	2.654(11)			
Al 10	–Ta 2	2.782(2)						
	–Ta 2	2.782(2)						
	–Ta 3	2.883(2)						
	–Ta 3	2.883(2)						
	–Ta 4	2.8990(19)						
	–Ta 4	2.8990(19)						
	–Ta 5	2.865(3)						
	–Ta 5	2.865(3)						
	–Ta 7	2.861(3)						
	–Ta 7	2.861(3)						
	–Ta 12	2.818(3)						
	–Ta 12	2.818(3)						

tantalum atom in 8*j* and the atoms in sites $8i_2$ and 2*a* become too short (even shorter if one considers the replacement of some aluminum on these sites of CN 12 by tantalum) and have to be relaxed by the *c* expansion.

Finally, anisotropic line broadening (*hk*0 lines larger than 00*l* lines) has been evidenced for the three single-phase samples. For the three compositions concerned, *c* is shown to be nearly constant as a function of the composition, while *a* increases strongly with Ta composition. Slight inhomogeneities may therefore result in broadened *h k* 0 lines as compared to 0 0 *l* lines, which is actually observed.

4.3. Phase diagram

This work allows to specify the Ta-rich part of the Ta–Al system. At 1460 °C, we have established that the width of the σ phase domain is from 60.1 to 76 at.% Ta. It is sensibly larger than the one assessed by Du and Schmid-Fetzer [8] (65–79 at.%) in the Ta-poor region. The discrepancy, as most of the discrepancies reported so far for this system, may be related to the nearly complete absence of EPMA results in previous work. The difficulty in controlling Al losses makes necessary the use of such an

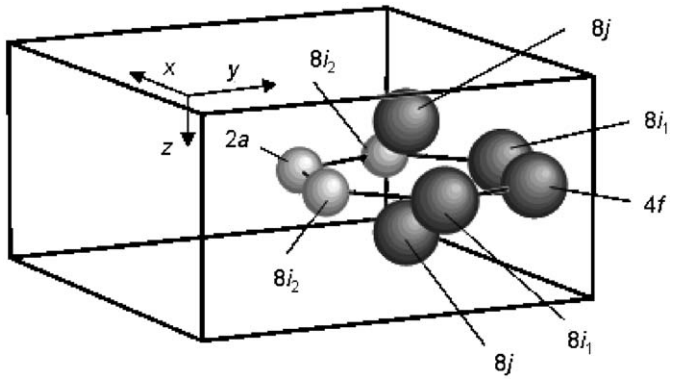

Fig. 6. Part of the structure of the σ phase explaining tentatively the increase of the c parameter when a decreases, see text (Ta in dark, Al in light).

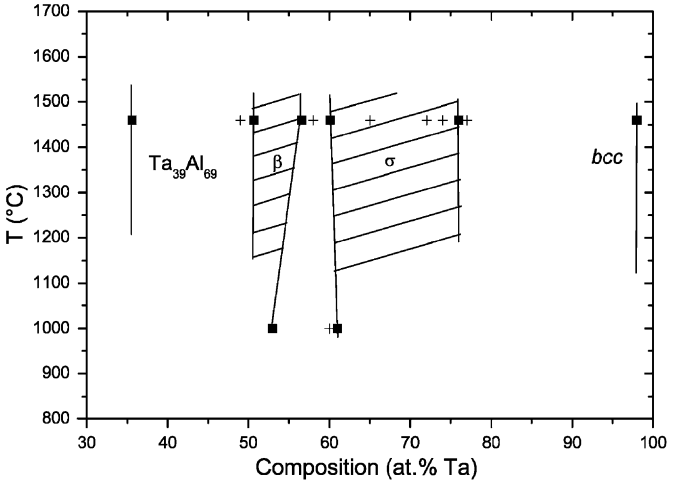

Fig. 7. Representation of the compositions studied and phase equilibria in the form of a phase diagram.

analytical technique. Another difference is the evidencing of the non-stoichiometric nature of the β phase and the presence of a homogeneity domain. A representation of the synthesized compositions and phase equilibria is given in the form of a schematic phase diagram in Fig. 7.

5. Conclusion

The Ta–Al system has been studied in the Ta-rich region. Phase equilibria have been accurately determined in terms of composition and nature of the phases involved. The two intermetallic phases present in this region have been structurally characterized. The nature and the location of the defects responsible for the presence of a large homogeneity domain for the σ phase have been studied by Rietveld analysis. The structure of the β phase has been solved ab initio from powder synchrotron data. This phase is very close to the group of Frank–Kasper phases to which belongs the σ phase.

Acknowledgments

The authors thank F. Briaucourt and K. Daoud for their participation in the synthesis and characterization, and E. Leroy for the EPMA measurements. Hermann Emerich from the Swiss–Norwegian Beamline at the ESRF is highly acknowledged for his help with the diffraction experiment.

References

[1] H. Nowotny, C. Brukl, F. Benesovsky, Monatsh. Chem. 92 (1961) 116–127.
[2] A. Raman, Aluminium 41 (1965) 318–319.
[3] J.C. Schuster, Z. Metallkd. 76 (11) (1985) 724–727.
[4] P.R. Subramanian, D.B. Miracle, S. Mazdiyasni, Met. Trans. A 21 (1990) 539–545.
[5] S. Mahne, F. Krumeich, B. Harbrecht, J. Alloys Compds. 201 (1993) 167–174.
[6] S. Mahne, B. Harbrecht, J. Alloys Compds. 203 (1994) 271–279.
[7] S. Mahne, B. Harbrecht, F. Krumeich, J. Alloys Compds. 218 (1995) 177–182.
[8] Y. Du, R. Schmid-Fetzer, J. Phase Equilibria 17 (4) (1996) 311–324.
[9] A.K. Sinha, Prog. Mater. Sci. 15 (1972) 79–185.
[10] E.O. Hall, S.H. Algie, Metall. Rev. 11 (1966) 61–88.
[11] J. Rodríguez-Carvajal, in: XV Congress of International Union of Crystallography, Satellite Meeting on Powder Diffraction, 1990, p. 127.
[12] V. Favre-Nicolin, R. Černý, J. Appl. Crystallogr. 35 (2002) 734–743.
[13] P.T. Moseley, C.J. Seabrook, Acta Crystallogr. B 29 (1973) 1170–1171.
[14] L.M. Alte Da Veiga, M.M.R.R. Costa, M.J.M. De Almeida, L.R. Andrade, A. Matos Beja, Acta Crystallogr. B 36 (1980) 1750–1757.
[15] L.-E. Edshammar, B. Holmberg, Acta Chem. Scand. 14 (5) (1960) 1219–1220.
[16] J.-M. Joubert, C. Pommier, E. Leroy, A. Percheron-Guégan, J. Alloys Compds. 356–357 (2003) 442–446.
[17] P.W. Brown, F.J. Worzala, J. Mater. Sci. 11 (1976) 760–766.
[18] C.G. Wilson, F.J. Spooner, J. Mater. Sci. 12 (1977) 1653–1658.